POLITECNICO DI TORINO
Repository ISTITUZIONALE

Hot isostatic pressing as a tool for enhancing the diffusion bonding of dissimilar materials using interference fitting as pre-joining technique

Original
Hot isostatic pressing as a tool for enhancing the diffusion bonding of dissimilar materials using interference fitting as pre-joining technique / Bassini, E., Tringali, N., Ugues, D.. - In: POWDER METALLURGY. - ISSN 0032-5899. - ELETTRONICO. - (2026), pp. 1-6. [10.1177/00325899261430114]

Availability:
This version is available at: 11583/3011795 since: 2026-06-08T14:49:10Z

Publisher:
Sage

Published
DOI:10.1177/00325899261430114

Terms of use:

This article is made available under terms and conditions as specified in the corresponding bibliographic description in the repository

Publisher copyright
Sage postprint/Author's Accepted Manuscript

(Article begins on next page)

13 September 2026

Hot Isostatic Pressing as a tool for enhancing the diffusion bonding of dissimilar material

Emilio Bassini [1*], Nino Tringali[1], Daniele Ugues[1]
[1]Politecnico di Torino C.so Duca degli Abruzzi 24, 10129 Torino, Italy

Summary – One nickel-based superalloy and austenitic stainless steel were joined together using a technique that didn't require any capsule or welding. The trial was performed with a low-pressure furnace and in a Hot Isostatic Press. The Press, a Quintus QIH 15 L, was coupled with the uniform rapid cooling module (URC) to join the two metals and deliver a suitable heat treatment for both alloys. In contrast to the low-pressure furnace, the application of the HIP effectively halved the processing time required for the joining procedure. This research highlights the critical roles of time and temperature in achieving a successful bond between the two dissimilar metals. The interface between the two metals was studied in depth with optical and electronic microscopy and EDS to assess better the solid-state diffusion of the involved elements.
Keywords: diffusion bonding, interface analysis, Microscopy, Hip Quench, heat treatment.

1 Introduction

Combining dissimilar materials using techniques beyond traditional welding is gaining increasing attention. Many industries, particularly nuclear power plants, require materials with distinct and often conflicting properties, achievable only by combining different materials. While this capability unlocks numerous opportunities, it also presents significant challenges. For instance, brittle phases may develop at the interface of joined materials, or cracks can form due to mismatched thermal expansion coefficients. These differences in material properties often act as barriers when using conventional joining methods. However, advanced techniques like diffusion bonding or hot isostatic pressing (HIP) diffusion bonding provide greater flexibility and enable innovative solutions to overcome these issues, even when steel is welded with a Ni-based superalloy.

Guo et al. [1] reported that currently, various methods are available for connecting superalloys, including fusion welding, brazing, friction bonding, and diffusion bonding. Among these, fusion welding techniques such as laser welding and electron beam welding are the most commonly used in aircraft engine manufacturing. However, joints produced by these methods are prone to liquefaction cracks. Similarly, transient liquid phase (TLP) bonding can introduce melting elements that lead to the formation of brittle and hard borides within the joint, compromising its performance.

On the other hand, diffusion bonding is considered one of the most suitable methods for joining superalloys due to its ability to minimize deformation and maintain the excellent high-temperature performance of superalloy components. Nevertheless, limitations still exist: for example, in the Haynes 230 alloy, solid-state diffusion bonding conducted at 4 MPa, 950 °C, and for 120 minutes resulted in Cr-rich precipitates at the joint interface, which hindered grain migration and caused unbonded areas and void defects. This condition highlights the tendency of nickel-based superalloys to resist deformation at high temperatures, leading to increased yield stress at the connection interface. Consequently, researchers have begun exploring diffusion bonding methods by adding interlayers to improve the bonding of

nickel-based superalloys [1]. An evolution of traditional diffusion bonding is HIP-assisted diffusion bonding, which effectively prevents macro-deformation during the bonding process while maintaining high dimensional accuracy, making it particularly well-suited for complex structures. This technique efficiently bonded FeCrAl and Reduced Activation Ferritic Martensitic steels (RAFM). In diffusion bonding joints, the closure of interfacial voids is a key factor in assessing bonding quality, as it directly influences the joint's mechanical properties [2]. Nevertheless, this technique requires a capsule to wrap the two components one wants to weld.

The temperatures employed in diffusion bonding remain below the melting points of the joined materials. The joints achieve exceptional strength and toughness through plastic deformation and elemental interdiffusion across the bonding interface. Hot Isostatic Pressing (HIP), an advanced diffusion bonding technique, uses inert gases as a medium to apply pressure. Researchers have successfully utilized HIP to directly join dissimilar metal alloys, such as SA508 low alloy steel and 316L stainless steel. During the HIP process, interdiffusion zones formed at both interfaces, with Cr and Ni diffusing from 316L to SA508 and Fe migrating from SA508 to 316L. This resulted in a robust diffused interface. The 316L/SA508 joint demonstrated an ultimate tensile strength of 612 MPa, with all tensile specimens failing on the 316L side, confirming the excellent interfacial strength [1,3]. Diffusion bonding is a promising technique for fabricating W/steel junctions. However, creating a reliable W/RAFM-steel joint is challenging due to the mismatch in the coefficients of thermal expansion (CTE) between W ($4.5 \times 10^{-6}\,K^{-1}$) and steel ($12–14 \times 10^{-6}\,K^{-1}$ at room temperature). This disparity generates significant residual thermal stress along the interface during cooling from the bonding temperature to room temperature and high thermal stress under surface heat loading. A practical solution to address both issues is the incorporation of soft pure metal interlayers between W and steel. These interlayers allow high thermal stress to be alleviated through plastic deformation and reduce the formation of W-steel reaction products by preventing direct contact between the two materials [4]. Many authors report that the surface condition is a critical factor in achieving a high-quality joint in solid HIP bonding. Surfaces often exhibit irregularities due to the machining process, resulting in surface cleanliness and roughness variations. Studies have demonstrated that these two factors, surface cleanliness and surface roughness, are key determinants of the quality of HIP-bonded joints [5]. In this work, diffusion and HIP diffusion bonding were explored, specifically avoiding pre-welding or encapsulation. The joint's tightness was ensured solely through geometrical interference between the two components. Although the geometries studied—a cylinder and a plate—were relatively simple, this initial investigation laid the groundwork for understanding the differences between low-pressure diffusion bonding of a Ni-based superalloy with an austenitic stainless steel and bonding achieved through Hot Isostatic Pressing (HIP). A subsequent gas quenching process was employed to prevent the formation of harmful particles in the adjoining metals. The study primarily focuses on evaluating the feasibility of the process, along with a detailed microstructural and chemical analysis of the resulting interface.

2 Materials and methods

The base materials for the joining process were AISI 310 stainless steel and 353 MA alloy. AISI 310 was supplied as an annealed cylindrical billet, while 353 MA, a Fe-Ni-based alloy with minor cerium additions, was also provided as a rolled plate in the annealed state. The nominal compositions of these materials were confirmed via

EDS spectroscopy, with key elements being chromium, nickel, and manganese, alongside controlled levels of carbon, silicon, and nitrogen. **Table 1** shows the chemical composition of the two metals used for the joining.

Table 1: Chemical composition of the metals used to create the joining

Element (% by weight)	Fe	C	Ni	Cr	Mn	Si	N	Ce
AISI 310	Bal.	0.25	21	25	2	1.5	-	-
353 MA	Bal.	0.07	35	25	1.5	1.6	0.16	0.05

AISI 310 was made into a cylindrical billet, and 353 MA was provided as a rolled plate. These materials were cut into specific geometries using a CNC milling machine. The final shape for the bonding samples consisted of a square base (5 mm thick) made from 353 MA and a 10 mm diameter cylinder from AISI 310 fitted into a hole of the same size in the base. The mechanical assembly process involved interference in the fitting of the parts. Interference fitting was employed to maximize the initial contact area between the materials and to prevent gas infiltration during subsequent Hot Isostatic Pressing (HIP). Before assembly, all parts were cleaned using ultrasonic baths in acetone to remove surface contaminants. After cleaning, the parts were heated to 250 °C in a modified Manfredi L2A air oven to achieve tight tolerances during the interference fitting.
A constant flux of Argon was applied to limit the oxidation of the plate. These steps ensured that the samples were adequately prepared for the diffusion bonding processes, either vacuum VDB or HIP DB, which were subsequently used for permanent bonding. **Figure 1** shows the joint from top view and its cross-section. The roughness of the samples was measured using a Hommelwerke Hommel tester T1000 profilometer. For the lateral surface of the cylinders, an average Ra value of 0.39 µm and an average Rq value of 0.48 µm were recorded. These roughness values were considered suitable for the diffusion bonding (DB) process. The values were judged similar also along the inner surface of the hole since all the parts were machined using the same tool. The roughness was kept within acceptable limits to facilitate the bonding process without further surface finishing.

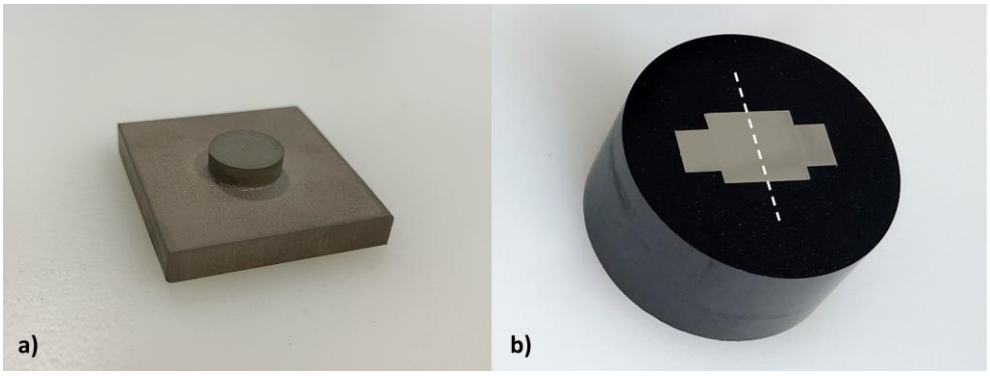

Figure 1: The Austenitic stainless steel and Ni-based coupled together before VDB or HIP DB from the top view a) and in cross section b).

The assembled parts were subjected to the VDB and HIP DB processes according to the following recipes. VDB was applied using a vacuum furnace (TAV type

MINIJET - HP), heating the samples to 1200 °C for 2 hours. This was followed by a cooling process at about 135 °C/min. Trials at lower temperatures were unsuccessful and thus not presented here. Hot Isostatic Pressing (HIP) Diffusion Bonding involved using the Quintus QIH-15L unit, with a pressure of 100 MPa during the bonding phase. Different temperatures were employed, ranging from 1100 to 1200 °C for 60 minutes applying 100 MPa and a cooling rate of ca.140°C/min All the tests were successful, so only the one performed at 1100°C is shown in detail since it has the most microstructural advantages. To prepare samples for optical and electron microscope observations, samples were cut from the as-received materials or the post-diffusion bonding samples using a metallographic cutting machine. The samples were then embedded in phenolic resin, ground and polished. Grinding was done using progressively finer abrasive papers up to a grit size of 2400, followed by polishing with diamond suspensions down to a 1 µm size. The etching was performed using electrochemical etching with a 20% water solution of H_3PO_4 at 3 V for 5-10 seconds. The post-diffusion bonding samples were observed both in the polished state and after electrolytic etching to assess the samples' morphology, residual porosity, and microstructure. A ZEISS EVO 15 scanning electron microscope (SEM) equipped with an Oxford Instruments Ultim Max EDS probe was used for electron microscopy. The goal was to assess the interface's chemical composition and microstructural characteristics, mainly focusing on grain migration and recrystallization during the bonding process. Finally, Vickers microhardness test was performed following ASTM E92-17 standards. The tests were conducted using a 25 gf load applied for 15 seconds at 43 different points near the bonding interface. This technique allowed for mapping the microhardness variation across the bonded interface, providing insights into the mechanical properties of the joint.

3 Results

Figure 2 shows the microstructure of AISI 310 and 353 MA in the as-received condition with equiaxial grains. AISI 310 has larger average grain sizes compared to 353 MA, with the first measuring 143 µm ± 15 and 65 µm ± 9 the latter, respectively.

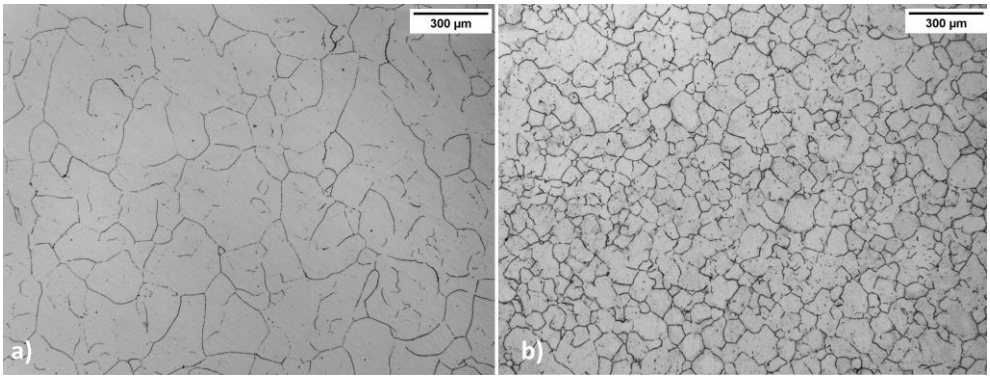

Figure 2: Microstructure of AISI 310 a) and 353 MA b) in the as-received conditions.

Figure 3 shows the joint after the VDB process. The picture shows the upper half portion of the joint as polished. The whole interface was assessed to evaluate the volume fraction of residual porosity. A detail of the interface is shown as well after etching. This was considered helpful for better evaluating the size and the shape of grains precisely at the interface position. Finally, EDS maps and line profiles for the

most important elements are reported to understand better how the elements' diffusion took place. The microstructure investigation demonstrated that only a limited grain migration across the interface occurred. Large pores (5-7 µm in diameter) were visible in the as-polished sample. Smaller grains were noticed on the 353 MA side, particularly near the interface, suggesting that localized recrystallization phenomena took place, probably due to the stress accumulated during the bonding process and coming from the very tight tolerances used. The heat treatment was performed at 1200 °C, causing a noticeable grain coarsening, especially in the AISI 310 half. The grains are 198 µm ± 15 and 140 ± 23 in the AISI 310 and 353 MA, respectively. The original interface position is evident with vertically oriented grain boundaries, which remained discernible, suggesting only partial integration at the microstructural level. Finally, some spherical Silicon reach oxides were detected near the interface, which could have been co-responsible for the limited migration of the grains past the interface.

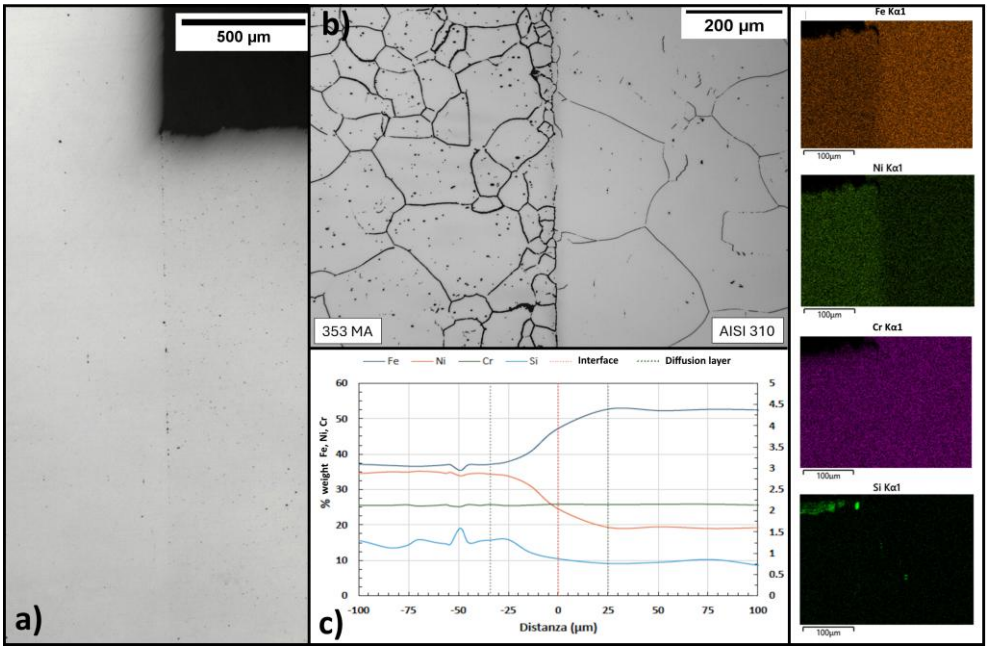

Figure 3: VDB sample observed as-polished with LOM a) and after etching b). The EDS profile is shown in c), while the EDS MAP is shown in the right column.

Regarding the elements' diffusional profile, the sample shows a diffusion layer of approximately 59 µm thick. This measurement was based on the changes in Fe and Ni concentrations until their nominal values were again reached. Naturally, iron was found in higher concentrations on the AISI 310 side, while Ni was dominant in the 353 MA alloy. On the other hand, Chromium concentrations remained almost constant across the interface due to its similar content in both base materials. Finally, Si showed localized peaks, likely indicative of oxidized species rich in this element. EDS Maps were particularly effective in locating silicon oxides at the interface. The fact that these oxides are spherical suggests that these particles were already contained in the base material, an inclusion coming from the steelmaking process. If oxidation had occurred during the VDB process, the oxidation would form a layer or

scale rather than spheres. **Figure 4** shows the sample after HIP DB, focusing on the same features. This sample was obtained using the HIP at only 1100 °C for 1 hour with a pressure of 100 MPa. The microstructural and chemical analysis evidenced that residual porosity was minimal and well below the level observed in the VDB sample. The few defects were always below 0.7 µm in diameter and located near the original interface. The lower temperature used allowed for lower grain coarsening. In particular, in the 353 MA region, the grains now measure 152 ± 9 and 74 ± 14 µm, respectively. Similarly to what happened in the VDB sample, finer grains were noticed at the interface. Still, this time, the smaller grains are visible in both the materials, suggesting that small recrystallization processes took place in both the alloys. The EDS profile evidenced a diffusion layer of ca. 60 µm, which is consistent with the former sample. On the other hand, no oxide was evidenced this time, which could be favorable for the correct interface development between the two metals. The maps and the line EDS confirm that strong element diffusion occurred during the process. Like the previous case, Chromium content was similar in the two base materials, therefore solid-state diffusion didn't occur, and the composition profile remained flat. On the other hand, despite the Silicon content being small, diffusion happened at the interface as well, indicating that, regardless of the element's concentration, diffusion will always occur if a chemical potential difference exists between the two metals.

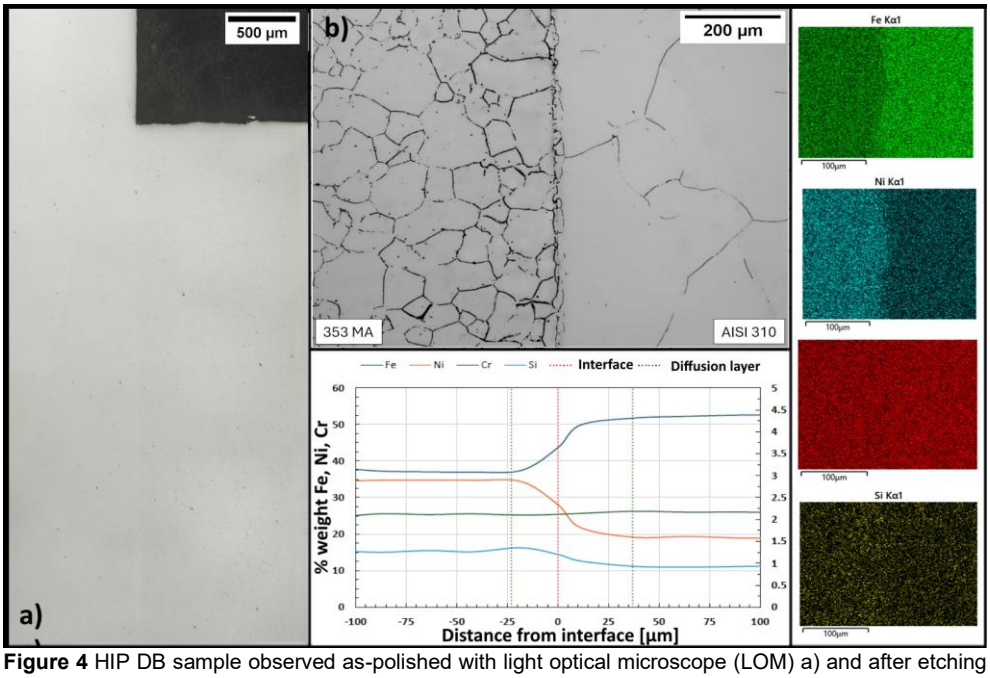

Figure 4 HIP DB sample observed as-polished with light optical microscope (LOM) a) and after etching b). The EDS profile is shown in c), while the EDS MAP is shown in the right column.

Figure 5 shows the micro-Vickers hardness grid used to assess the material hardness across the interface of the HIP DB sample. Microhardness maps,

performed applying 25gf, were created using data from low-load indentations near the junction areas of diffusion-bonded samples.

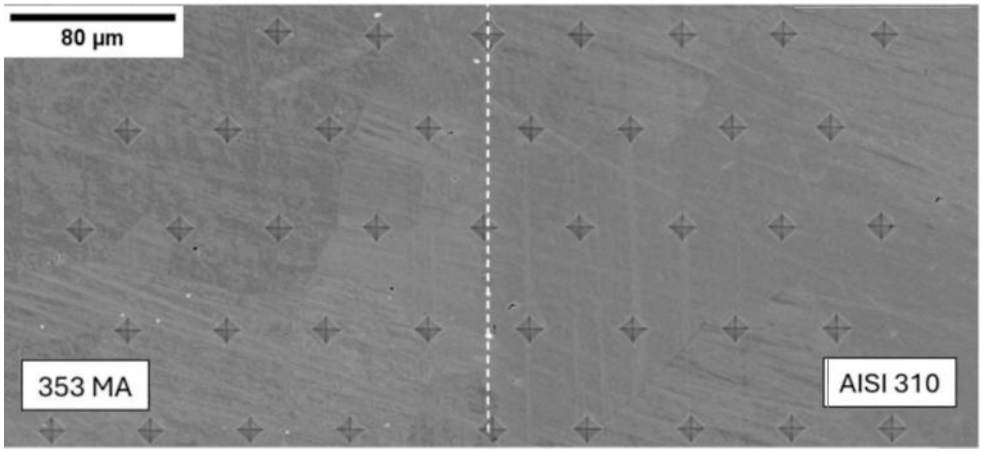

Figure 5: HIP DB sample after undergoing microvickers assessment

Measurements of indentation diagonals were performed using SEM images processed with ImageJ software, while the resulting contour map is shown in **Figure 6**. The grid is made by an 8 by 5 imprint set covering both the joint halves with 3 imprints falling precisely on the joint interface. The grid helped evidence the differences between the VDB and the HIP DB samples. VDB and HIP DB samples didn't show any crack opening or failure around the imprints performed at the interface, indicating a solid junction was achieved.

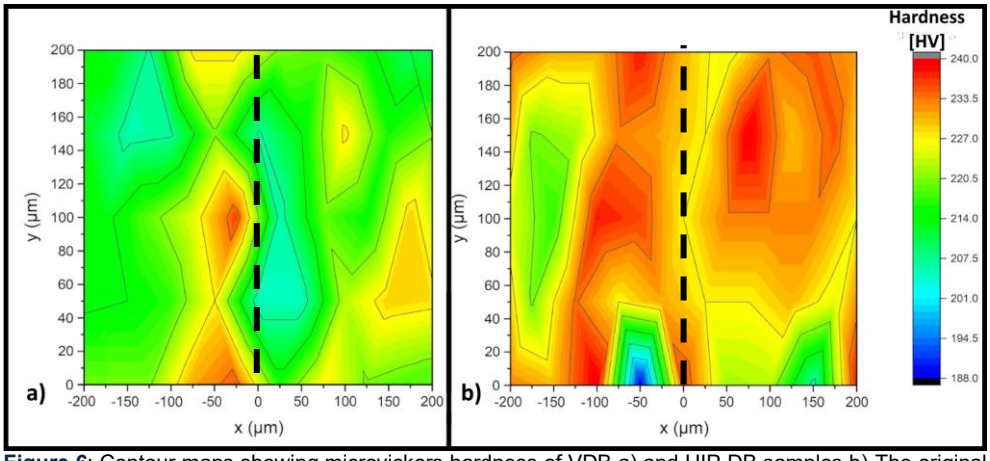

Figure 6: Contour maps showing microvickers hardness of VDB a) and HIP DB samples b).The original position of the interface is indicated by a black dashed line.

The two maps show that VDB samples have a lower hardness than the HIP DB one. The main reason for the difference is the grain size achieved during the two treatments. The HIP DB sample required a lower temperature to complete the joint, limiting the grain coarsening and thus maintaining the average hardness level, which was 20 points higher than the VDB sample. At the same time, slightly lower hardness values were recorded near the interface, but this could be derived from the limited

number of indentations effectively falling at the interface. On the other hand, the hardness drop for the VDB sample is much more evident, and the hot spot (in red) was likely due to indentation on the SiO_2 particles previously described.

4 Conclusions

This study evaluated the feasibility of solid-state bonding between dissimilar materials, AISI 310 stainless steel and 353 MA alloy, without relying on traditional encapsulation or welding methods. The findings highlight that Vacuum Diffusion Bonding (VDB) and Hot Isostatic Press Diffusion Bonding (HIP DB) can create joints without melting the base materials, thereby minimizing thermally affected zones and preserving the microstructure. However, certain limitations were identified. VDB requires very high temperatures (at least 1200 °C) to achieve a sound bond, which can lead to excessive grain growth and a reduction in mechanical properties. In contrast, HIP DB demonstrated effectiveness at lower temperatures (1100 °C) due to applying 100 MPa isostatic pressure even for shorter application time. Furthermore, the study confirmed that the geometrical tolerances used were sufficient to prevent argon leakage at the interface, a critical factor for ensuring the viability of HIP DB. Nonetheless, the simplicity of the geometries employed in this work must be considered when scaling the technique for more complex applications.

References

[1] W. Guo, J. Xin, D. Hao, Y. Ma, J. Xiong, J. Li, Q. Feng, Diffusion bonding of nickel-based powder metallurgy superalloy FGH98 with pure nickel interlayer, Journal of Materials Research and Technology 30 (2024) 267–282. https://doi.org/10.1016/J.JMRT.2024.03.082.

[2] P.S. Du, W.J. Wang, J.C. Wang, H.Q. Xu, Q. ling Wang, Z.Y. Yu, W. jing Zhang, H. Chen, W. Liu, Y.P. Xu, H.S. Zhou, G.N. Luo, Evolution of interface voids and columnar grains of the FeCrAl/RAFMs HIP bonding joint, Materials Science and Engineering: A 915 (2024) 147287. https://doi.org/10.1016/J.MSEA.2024.147287.

[3] H. Zheng, C. Cai, R. Guo, Y. Shi, Diffusion bonding among hard alloy, tool steel, and alloy steel by hot isostatic pressing: Interfacial microstructure and mechanical properties, Int J Refract Metals Hard Mater 118 (2024) 106478. https://doi.org/10.1016/J.IJRMHM.2023.106478.

[4] P. Huang, Y. Wang, H. Peng, J. Chen, P. Wang, Diffusion bonding W and RAFM-steel with an Fe interlayer by hot isostatic pressing, Fusion Engineering and Design 158 (2020) 111796. https://doi.org/10.1016/J.FUSENGDES.2020.111796.

[5] Y. Zhao, C. Li, B. Huang, S. Liu, Q. Huang, Verification of the effect of surface preparation on Hot Isostatic Pressing diffusion bonding joints of CLAM steel, Journal of Nuclear Materials 455 (2014) 486–490. https://doi.org/10.1016/J.JNUCMAT.2014.08.004.